

1-2013

## Analysis of L1C Acquisition by Combining Pilot and Data Components over Multiple Code Periods

Kelly C. Seals

William R. Michalson

Peter F. Swaszek

*University of Rhode Island, swaszek@uri.edu*

Richard J. Hartnett

Follow this and additional works at: [https://digitalcommons.uri.edu/ele\\_facpubs](https://digitalcommons.uri.edu/ele_facpubs)

---

### Citation/Publisher Attribution

Seals, Kelly C., Michalson, William R., Swaszek, Peter F., Hartnett, Richard J., "Analysis of L1C Acquisition by Combining Pilot and Data Components over Multiple Code Periods," *Proceedings of the 2013 International Technical Meeting of The Institute of Navigation*, San Diego, California, January 2013, pp. 526-535.

Available at: <http://www.ion.org/publications/abstract.cfm?jp=p&articleID=10863>

This Conference Proceeding is brought to you by the University of Rhode Island. It has been accepted for inclusion in Electrical, Computer, and Biomedical Engineering Faculty Publications by an authorized administrator of DigitalCommons@URI. For more information, please contact [digitalcommons-group@uri.edu](mailto:digitalcommons-group@uri.edu). For permission to reuse copyrighted content, contact the author directly.

---

## Analysis of L1C Acquisition by Combining Pilot and Data Components over Multiple Code Periods

Terms of Use

All rights reserved under copyright.

# Analysis of L1C Acquisition by Combining Pilot and Data Components over Multiple Code Periods

Kelly C. Seals, *U.S. Coast Guard Academy*  
William R. Michalson, *Worcester Polytechnic Institute*  
Peter F. Swaszek, *University of Rhode Island*  
Richard J. Hartnett, *U.S. Coast Guard Academy*

## BIOGRAPHIES

Kelly C. Seals is a member of the Electrical Engineering faculty at the U.S. Coast Guard Academy and a Ph.D. student at Worcester Polytechnic Institute.

William R. Michalson is a Professor in the ECE Department at the Worcester Polytechnic Institute where he performs research and teaches in the areas of navigation, communications and computer system design. He supervises the WPI Center for Advanced Integrated Radio Navigation (CAIRN).

Peter F. Swaszek is a Professor in the Department of Electrical, Computer, and Biomedical Engineering at the University of Rhode Island. His research interests are in statistical signal processing with a focus on digital communications and electronic navigation systems.

Richard J. Hartnett is a Professor in Electrical Engineering at the U.S. Coast Guard Academy. His research interests include efficient digital filtering techniques for electronic navigation systems and autonomous ground vehicle design.

## ABSTRACT

One of the new features of modern GNSS signals is that they generally have a pilot component and data component. A unique aspect of the GPS L1C signal is that it has an unequal power split between the pilot and data components. Various papers have proposed channel combining techniques to acquire modern GNSS signals using both components.

In this paper, the optimal detector for GPS L1C acquisition over multiple code periods without knowledge of the navigation data or overlay code phase is derived. A variation of semi-coherent integration technique (non-coherently combining the 10 msec coherent combinations) that accounts for the unequal power split between the data and pilot components is proposed. Single trial detection and false alarm probabilities are

used to compare performance of this semi-coherent integration with unequal power compensation to the optimal detector as well as to noncoherent combining and single channel acquisition on the pilot component only. Simulation results show that the semi-coherent integration with unequal power compensation slightly outperforms both the semi-coherent integration detector without compensating for unequal power and the noncoherent combining detector.

## INTRODUCTION

L1C is the most recent of the modernized GPS signals with the first launch of a GPS Block III satellite with this signal payload expected to occur within a few years. One of the interesting features of modern Global Navigation Satellite System (GNSS) signals, including the GPS L1C signal, is the presence of data and pilot components. The pilot component is a carrier with a deterministic overlay code but no data symbols whereas the data component carries the navigation data symbol stream. Two unique aspects of GPS L1C are the asymmetrical power split between the two components (75%/25% for the pilot/data) and the transmission of both components in phase with orthogonality achieved by code division multiplexing.

Unassisted acquisition of GNSS signals requires a two-dimensional search for code delay and Doppler frequency of the incoming signal. For modern two-component GNSS signals, conventional GNSS acquisition schemes could be used on either component, correlating the received signal with either the pilot or the data spreading code [1-3]. One obvious disadvantage of this approach is the wasting of signal power; hence, new techniques for signal combining or joint acquisition of the pilot and data components have been proposed.

Noncoherent combining, or acquisition of each component separately and combining the power from the correlators for each component was proposed in [4] and has been analyzed in various papers [3,5]. A technique

known as coherent channel combining with sign recovery takes advantage of the fact that the relative sign between the data and pilot components can be estimated by correlating the received signal with two different composite codes: the data spreading code plus the pilot spreading code and the pilot spreading code minus the data spreading code [3, 5–8]. Semi-coherent integration refers to noncoherently combining these coherent combinations (every 10 msec code period for the case of GPS L1C). Expressions for the single trial false alarm and detection probabilities for a single code period were derived in [3] for two-component GNSS signals transmitted in phase quadrature with equal power split and in [9] for signals in phase with unequal power split. Results were extended for using multiple code periods for the in phase quadrature signal with equal power split in [10].

In this paper, a brief introduction to the GPS L1C signal is first provided along with the signal model. The optimal detector for acquisition of the GPS L1C signal in an additive white Gaussian noise using an arbitrary integer number of primary code periods is derived. Single channel acquisition on the pilot only and noncoherent combining acquisition techniques are provided for comparison purposes. The semi-coherent combining technique for the GPS L1C signal is developed. Simulation results compare the performance of the optimal detector with single channel, noncoherent combining and semi-coherent combining acquisition techniques.

## GPS L1C AND SIGNAL MODEL

The design of the new civil signal in the L1 band, called L1C, was initiated in August 2003 and completed in April 2006 and is described in [11, 12]. It has the same carrier frequency of 1575.42 MHz as the legacy L1 C/A code signal but many innovative design features separate this signal from its counterpart on the same frequency that was designed thirty years prior. As the most recent of the modernized GPS signals, L1C has acquired many advancements seen in other modern signals including WAAS, L5, and L2C. The signal design for L1C is specified in the Interface Specification document IS-GPS-800A [13].

The L1C signal is split into two components with 75% power in the pilot component and 25% power in the data component. Spreading codes with a length of 10,230 chips and a period of 10 ms at a chipping rate of 1.023 Mcps are based on Weil codes [14]. Not only does each satellite have unique spreading codes, but different codes are also used for the pilot and data components. In addition to the spreading code, the pilot component uses an 18 second 1800-bit overlay

code. One bit of this overlay code and one bit of the navigation data on the data component both have a duration of 10 ms which corresponds to one period of the spreading code.

Both components of the L1C signal use binary offset carrier (BOC) modulation which is explained in [15]. BOC modulation uses a square-wave spreading symbol (subcarrier) to modulate each chip of the spreading code which splits the spectrum about the carrier frequency. The convention of using  $\text{BOC}(\alpha, \beta)$  to describe a BOC modulated symbol has become standard where the subcarrier frequency is  $f_s = \alpha \times 1.023$  MHz and the spreading code rate is  $f_c = \beta \times 1.023$  MHz. The modulation for the L1C data component is strictly  $\text{BOC}(1,1)$ . The L1C pilot component uses a time multiplexed combination of  $\text{BOC}(6,1)$  and  $\text{BOC}(1,1)$  known as TMBOC.

After signal conditioning in the front end of the GNSS receiver, the L1C signal from one satellite is

$$s(t) = \left[ \sqrt{\frac{3}{2}} C d_P(t - \tau) c_P(t - \tau) g_P(t - \tau) \cdot \cos(2\pi(f_{IF} + f_d)t + \delta\theta) \right] + \left[ \sqrt{\frac{1}{2}} C d_D(t - \tau) c_D(t - \tau) g_D(t - \tau) \cdot \cos(2\pi(f_{IF} + f_d)t + \delta\theta) \right] + n(t) \quad (1)$$

where

- where the total signal power is denoted as  $C$  (Watts) which includes any antenna gain and receiver implementation losses,
- $d_P(t)$  and  $d_D(t)$  are the series of overlay code and data bits,
- $c_P(t)$  and  $c_D(t)$  are the spreading codes for the pilot and data components,
- $g_P(t)$  and  $g_D(t)$  are the periodic repetition of the spreading symbols (also known as the subcarrier) for the data and pilot components and repeat every code chip,
- $\tau$  and  $f_d$  are the unknown delay and Doppler frequency of the signal,
- the signal is at an intermediate frequency  $f_{IF}$  (Hertz),
- the unknown phase term is  $\delta\theta$  (radians), which is the phase difference between the received signal and the locally generated signal used for down-conversion,
- and  $n(t)$  is additive white Gaussian noise with power spectral density  $N_0/2$ .

Despite being a discrete-time signal as this point in the receiver, continuous-time signals are used here to provide insight under the assumption that the sample-rate has been selected fast enough to accurately represent the signal.

After multiplication by two reference signals that are in phase quadrature and subsequent low-pass filtering, the inphase and quadrature channels are

$$\begin{aligned} \text{I - Channel} = & \\ & \sqrt{\frac{3}{4}} C d_P(t - \tau) c_P(t - \tau) g_P(t - \tau) \cos(2\pi \Delta f_d t + \Delta \theta) \\ & + \sqrt{\frac{1}{4}} C d_D(t - \tau) c_D(t - \tau) g_D(t - \tau) \cos(2\pi \Delta f_d t + \Delta \theta) \\ & + n_I(t) \end{aligned} \quad (2)$$

$$\begin{aligned} \text{Q - Channel} = & \\ & \sqrt{\frac{3}{4}} C d_P(t - \tau) c_P(t - \tau) g_P(t - \tau) \sin(2\pi \Delta f_d t + \Delta \theta) \\ & + \sqrt{\frac{1}{4}} C d_D(t - \tau) c_D(t - \tau) g_D(t - \tau) \sin(2\pi \Delta f_d t + \Delta \theta) \\ & + n_Q(t), \end{aligned} \quad (3)$$

where  $\Delta f_d = f_d - \hat{f}_d$  is the error in Doppler estimate and  $\Delta \theta = \theta - \hat{\theta}$  is the carrier phase offset between the local replica and received signal.

The inphase and quadrature channels are coherently integrated after each are multiplied by the local code and spreading symbol (subcarrier) replicas. This gives the scalar output of the I-channel and Q-channel correlators for both the pilot and data components every integer multiple of the coherent integration time,  $kT_c$ :

$$\begin{aligned} I_{P,k} &= \frac{\sqrt{\frac{3}{4}} C d_{P,k}}{T_c} \int_{kT_c}^{kT_c+T_c} c_P(t-\tau) c_P(t-\hat{\tau}) g_P(t-\tau) \\ &\quad \cdot g_P(t-\hat{\tau}) \cos(2\pi \Delta f_d t + \Delta \theta) dt + \eta_{P,I,k} \\ Q_{P,k} &= \frac{\sqrt{\frac{3}{4}} C d_{P,k}}{T_c} \int_{kT_c}^{kT_c+T_c} c_P(t-\tau) c_P(t-\hat{\tau}) g_P(t-\tau) \\ &\quad \cdot g_P(t-\hat{\tau}) \sin(2\pi \Delta f_d t + \Delta \theta) dt + \eta_{P,Q,k} \\ I_{D,k} &= \frac{\sqrt{\frac{1}{4}} C d_{D,k}}{T_c} \int_{kT_c}^{kT_c+T_c} c_D(t-\tau) c_D(t-\hat{\tau}) g_D(t-\tau) \\ &\quad \cdot g_D(t-\hat{\tau}) \cos(2\pi \Delta f_d t + \Delta \theta) dt + \eta_{D,I,k} \\ Q_{D,k} &= \frac{\sqrt{\frac{1}{4}} C d_{D,k}}{T_c} \int_{kT_c}^{kT_c+T_c} c_D(t-\tau) c_D(t-\hat{\tau}) g_D(t-\tau) \\ &\quad \cdot g_D(t-\hat{\tau}) \sin(2\pi \Delta f_d t + \Delta \theta) dt + \eta_{D,Q,k}, \end{aligned} \quad (4)$$

where  $T_c$  is the coherent integration time,  $\hat{\tau}$  is the estimated delay and  $\eta$  are the uncorrelated noise terms that each have the same variance,  $\sigma^2 = N_0/2T_c$  [16]. We assume that the coherent integration time the length of a of the spreading code period which is the

same as an overlay or data code bit (10 ms for GPS L1C) and that bit transitions are avoided. When the signal from the satellite is present and correct delay ( $\hat{\tau} = \tau$ ) and Doppler estimates are used, the output of the correlators are now

$$\begin{aligned} I_{P,k} &= \sqrt{\frac{3}{4}} C d_{P,k} \cos(\Delta \theta) + \eta_{P,I,k} \\ Q_{P,k} &= \sqrt{\frac{3}{4}} C d_{P,k} \sin(\Delta \theta) + \eta_{P,Q,k} \\ I_{D,k} &= \sqrt{\frac{1}{4}} C d_{D,k} \cos(\Delta \theta) + \eta_{D,I,k} \\ Q_{D,k} &= \sqrt{\frac{1}{4}} C d_{D,k} \sin(\Delta \theta) + \eta_{D,Q,k}. \end{aligned} \quad (5)$$

Due to the autocorrelation properties of the spreading code, the correlator outputs contain the noise terms only when incorrect delay estimates ( $\hat{\tau} \neq \tau$ ) are used.

## OPTIMAL DETECTOR FOR ACQUISITION OF GPS L1C

In this section, classical detection theory is used to derive the optimal detector for an arbitrary integer number of primary spreading code periods of the GPS L1C signal and in general, any two-component GNSS signal in which the components are in phase but have an unequal power split. The optimal detector for GPS L5 acquisition was derived in [5]. The optimal detector for GPS L1C acquisition over a single spreading code period was derived in [9] and the results are extended here to find the optimal detector for GPS L1C over multiple code periods.

In GNSS acquisition, there are two choices when trying to acquire the signal from a particular satellite: either the satellite signal is present or not. These hypotheses are formally defined as  $H_1$  when the satellite signal is present and  $H_0$  which corresponds to no satellite signal.

The output of the correlators are used here as the observation since they are sufficient statistics for detecting the signal in an additive white Gaussian noise channel [17, 18]. Correlator outputs for the L1C signal are derived in equation (4) and given in equation (5) for correct estimation of delay and Doppler. Due to autocorrelation properties of the codes, we assume that the correlator outputs contain noise only if an incorrect delay estimate is used. The observation vector at the output of the correlators under each of these two hypotheses are

$$\begin{aligned} H_1 : \mathbf{r} &= \begin{bmatrix} \mathbf{I}_P \\ \mathbf{Q}_P \\ \mathbf{I}_D \\ \mathbf{Q}_D \end{bmatrix} + \mathbf{n} = \begin{bmatrix} \sqrt{\alpha C} \mathbf{d}_P \cos(\Delta \theta) \\ \sqrt{\alpha C} \mathbf{d}_P \sin(\Delta \theta) \\ \sqrt{\beta C} \mathbf{d}_D \cos(\Delta \theta) \\ \sqrt{\beta C} \mathbf{d}_D \sin(\Delta \theta) \end{bmatrix} + \mathbf{n} \\ H_0 : \mathbf{r} &= \mathbf{n}. \end{aligned} \quad (6)$$

We observe  $K$  spreading code periods. Under  $H_1$ , the observation is the  $4K \times 1$  vector of correlator outputs from the  $K \times 10$  millisecond observation. The  $4K \times 1$  noise vector,  $\mathbf{n}$ , is white and Gaussian with covariance  $\sigma^2 \mathbf{I}$ , where  $\mathbf{I}$  is the identity matrix and  $\sigma^2 = N_0 / (2T_c)$  [16]. The received signal power is  $C$  with the parameters  $\alpha$  and  $\beta$  describing the power split between the two components so that  $\alpha + \beta = 1$ . For the GPS L1C signal,  $\alpha = 3/4$  and  $\beta = 1/4$ . The carrier phase residual (or phase offset between the local replica and received signal) is  $\Delta\theta$ . Each component may have data,  $d_P$  or  $d_D$ , which represents any navigation data, overlay code, or combination of these two items that might be present. These data vectors,  $\mathbf{d}_P$  or  $\mathbf{d}_D$ , are each  $K \times 1$  vectors which represent the data bit during each code period.

Since the a priori probabilities of a signal being present are unknown, the Neyman-Pearson criterion is used so that a test is designed to maximize the probability of detection ( $P_d$ ) under a particular probability of false alarm constraint ( $P_f$ ). The optimum test consists of using the observation  $\mathbf{r}$  to find the likelihood ratio  $\Lambda(\mathbf{r})$  and comparing this result to a threshold to make a decision [17]. The likelihood ratio is a ratio of conditional joint probabilities and is therefore a scalar:

$$\Lambda(\mathbf{r}) \triangleq \frac{p(\mathbf{r} | H_1)}{p(\mathbf{r} | H_0)}. \quad (7)$$

The likelihood ratio test is

$$\Lambda(\mathbf{r}) \underset{H_0}{\overset{H_1}{\gtrless}} TH, \quad (8)$$

where the threshold,  $TH$ , is determined as follows for a fixed  $P_f$ :

$$P_f = \int_{TH}^{\infty} p(\Lambda | H_0) d\Lambda. \quad (9)$$

The joint probability density function of  $\mathbf{r}$  is expressed as a product of the marginal probability density functions since all of the noise terms are mutually uncorrelated and therefore statistically independent zero-mean Gaussian random variables. The joint probability density function under hypothesis  $H_0$  (no satellite signal present) is

$$p(\mathbf{r} | H_0) = \left( \frac{1}{(2\pi)^2 \sigma^4} \right)^K \exp\left( \frac{-|\mathbf{r}|^2}{2\sigma^2} \right). \quad (10)$$

The joint probability density function under hypothe-

sis  $H_1$  (satellite signal is present) is

$$\begin{aligned} p(\mathbf{r} | H_1) &= \left[ \frac{1}{(2\pi)^2 \sigma^4} \right]^K \exp\left[ \frac{1}{2\sigma^2} \left| \mathbf{r} - e^{j\Delta\theta} \begin{bmatrix} \sqrt{\alpha C} \mathbf{d}_P \\ \sqrt{\beta C} \mathbf{d}_D \end{bmatrix} \right|^2 \right] \\ &= \left[ \frac{1}{(2\pi)^2 \sigma^4} \right]^K \exp\left( \frac{-p^2}{2\sigma^2} \right), \end{aligned} \quad (11)$$

where

$$\begin{aligned} p^2 &= |\mathbf{r}|^2 + KC \\ &\quad - 2\sqrt{C} \cos(\Delta\theta) \sum_{k=1}^K \left( \sqrt{\alpha} I_{P,k} d_{P,k} + \sqrt{\beta} I_{D,k} d_{D,k} \right) \\ &\quad - 2\sqrt{C} \sin(\Delta\theta) \sum_{k=1}^K \left( \sqrt{\alpha} Q_{P,k} d_{P,k} + \sqrt{\beta} Q_{D,k} d_{D,k} \right) \end{aligned} \quad (12)$$

By substituting equation (12) into equation (11) for  $p^2$ , the joint probability density function is now

$$\begin{aligned} p(\mathbf{r} | H_1) &= \left[ \frac{1}{(2\pi)^2 \sigma^4} \right]^K \exp\left( \frac{-|\mathbf{r}|^2}{2\sigma^2} \right) \exp\left( \frac{-KC}{2\sigma^2} \right) \\ &\quad \cdot \exp\left( \frac{\sqrt{C}}{\sigma^2} \cos(\Delta\theta) \sum_{k=1}^K \left( \sqrt{\alpha} I_{P,k} d_{P,k} + \sqrt{\beta} I_{D,k} d_{D,k} \right) \right) \\ &\quad \cdot \exp\left( \frac{\sqrt{C}}{\sigma^2} \sin(\Delta\theta) \sum_{k=1}^K \left( \sqrt{\alpha} Q_{P,k} d_{P,k} + \sqrt{\beta} Q_{D,k} d_{D,k} \right) \right). \end{aligned} \quad (13)$$

Since the carrier phase residual ( $\Delta\theta$ ), overlay code bit ( $d_P$ ), and data bit ( $d_D$ ), are unknown, we consider each of them a random variable with a known a priori density. The conditional probability density functions in the likelihood ratio can be found by averaging  $p(\mathbf{r} | H_0, \theta, d_P, d_D)$  and  $p(\mathbf{r} | H_1, \theta, d_P, d_D)$  over the probability density function of the random carrier phase residual and the probability mass function of the random bits:

$$\begin{aligned} p(\mathbf{r} | H_1) &= \sum_{\mathbf{d}_P, \mathbf{d}_D \in \{B\}} p(\mathbf{d}_P, \mathbf{d}_D) \\ &\quad \cdot \int_0^{2\pi} p(\mathbf{r} | H_1, \Delta\theta, d_P, d_D) p(\Delta\theta | H_1) d\Delta\theta \\ p(\mathbf{r} | H_0) &= \sum_{\mathbf{d}_P, \mathbf{d}_D \in \{B\}} p(\mathbf{d}_P, \mathbf{d}_D) \\ &\quad \cdot \int_0^{2\pi} p(\mathbf{r} | H_0, \Delta\theta, d_P, d_D) p(\Delta\theta | H_0) d\Delta\theta, \end{aligned} \quad (14)$$

where  $B$  represents all possible combinations of the data and pilot bits over the observation interval.

The likelihood ratio is now

$$\begin{aligned}
\Lambda(\mathbf{r}) &= \frac{p(\mathbf{r} | H_1)}{p(\mathbf{r} | H_0)} \\
&= \sum_{\mathbf{d}_P, \mathbf{d}_D \in \{B\}} p(\mathbf{d}_P, \mathbf{d}_D) \\
&\quad \frac{1}{2\pi} \int_0^{2\pi} \left[ \left[ \frac{1}{(2\pi)^2 \sigma^4} \right]^K \exp\left(\frac{-|\mathbf{r}|^2}{2\sigma^2}\right) \exp\left(\frac{-KC}{2\sigma^2}\right) \right. \\
&\quad \cdot \exp\left(\frac{\sqrt{C}}{\sigma^2} \cos(\Delta\theta) \sum_{k=1}^K \left(\sqrt{\alpha} I_{P,k} d_{P,k} + \sqrt{\beta} I_{D,k} d_{D,k}\right)\right) \\
&\quad \cdot \exp\left(\frac{\sqrt{C}}{\sigma^2} \sin(\Delta\theta) \sum_{k=1}^K \left(\sqrt{\alpha} Q_{P,k} d_{P,k} + \sqrt{\beta} Q_{D,k} d_{D,k}\right)\right) \\
&\quad \left. \cdot ((2\pi)^2 \sigma^4)^K \exp\left(\frac{+|\mathbf{r}|^2}{2\sigma^2}\right) \right] d\Delta\theta \\
&= \exp\left(\frac{-KC}{2\sigma^2}\right) \sum_{\mathbf{d}_P, \mathbf{d}_D \in \{B\}} p(\mathbf{d}_P, \mathbf{d}_D) \\
&\quad \cdot \frac{1}{2\pi} \int_0^{2\pi} \exp\left(\frac{\sqrt{C}}{\sigma^2} \cos(\Delta\theta) (x)\right) \\
&\quad \cdot \exp\left(\frac{\sqrt{C}}{\sigma^2} \sin(\Delta\theta) (y)\right) d\Delta\theta \tag{15}
\end{aligned}$$

where

$$\begin{aligned}
x &= \sum_{k=1}^K \left(\sqrt{\alpha} I_{P,k} d_{P,k} + \sqrt{\beta} I_{D,k} d_{D,k}\right), \\
y &= \sum_{k=1}^K \left(\sqrt{\alpha} Q_{P,k} d_{P,k} + \sqrt{\beta} Q_{D,k} d_{D,k}\right). \tag{16}
\end{aligned}$$

Since the first exponential function in (15) is not a function of the observable, the carrier phase offset or overlay/data bits, we can incorporate it into the threshold so that the likelihood ratio for the optimal GPS L1C detector is now

$$\begin{aligned}
\Lambda(\mathbf{r}) &= \sum_{\mathbf{d}_P, \mathbf{d}_D \in \{B\}} p(\mathbf{d}_P, \mathbf{d}_D) \\
&\quad \frac{1}{2\pi} \int_0^{2\pi} \left[ \exp\left(\frac{\sqrt{C}}{\sigma^2} \cos(\Delta\theta) (x)\right) \right. \\
&\quad \left. \cdot \exp\left(\frac{\sqrt{C}}{\sigma^2} \sin(\Delta\theta) (y)\right) \right] d\Delta\theta \\
&= \sum_{\mathbf{d}_P, \mathbf{d}_D \in \{B\}} p(\mathbf{d}_P, \mathbf{d}_D) \\
&\quad I_0\left(\frac{\sqrt{C}}{\sigma^2} \sqrt{x^2 + y^2}\right), \tag{17}
\end{aligned}$$

where  $I_0$  is the modified Bessel function of zeroth order and  $x, y$  are defined in equation (16). This is similar to the optimal detector for acquisition of the GPS L5

signal derived in [5]. The optimal GPS L1C detector presented here however, includes scale factors based on the power split between the data and pilot components as well as different ordering of terms due to the components being in phase as opposed to in phase quadrature.

## SINGLE CHANNEL ACQUISITION

Either the pilot or data component can be used for acquisition for two-component GNSS signals. Since the phase of the carrier is unknown, the conventional noncoherent detection algorithm squares the output of the correlators and adds them together to get the decision variable, which in the case of acquisition of the pilot component is:

$$Z = \sum_{k=1}^K (I_{P,k}^2 + Q_{P,k}^2). \tag{18}$$

Since the correlator outputs are Gaussian random variables, the decision variable  $Z$  is a chi-square random variable with  $2K$  degrees of freedom. When incorrect delay and Doppler estimates are used, the correlator outputs are zero mean so that  $Z$  has a central chi-square distribution. However, when correct delay and Doppler values are used,  $Z$  is a noncentral chi-square random variable with noncentrality parameter

$$a_{scp}^2 = \frac{3}{4} KC. \tag{19}$$

When the value of the decision variable  $Z$  is above a threshold  $\lambda$ , the signal is considered present. In the acquisition process, there are two hypotheses formally defined as  $H_1$  when the satellite signal is present and  $H_0$  which corresponds to no satellite signal. Performance of the acquisition scheme can be determined by how often a signal is declared present when it actually is not which is known as the false alarm probability ( $P_{fa}$ ) and how often the signal is declared present correctly which is known as the detection probability ( $P_d$ ). Since  $Z$  is a chi-square random variable, these two probabilities are well known:

$$\begin{aligned}
P_{fa}^{scp}(\lambda) &= P(Z > \lambda | H_0) \\
&= 1 - P(Z < \lambda | H_0) \\
&= \exp\left(\frac{-\lambda}{2\sigma^2}\right) \sum_{k=0}^{K-1} \frac{1}{k!} \left(\frac{\lambda}{2\sigma^2}\right)^k \tag{20}
\end{aligned}$$

and

$$\begin{aligned}
P_d^{scp}(\lambda) &= P(Z > \lambda | H_1) \\
&= 1 - P(Z < \lambda | H_1) = Q_K\left(\frac{a_{scp}}{\sigma}, \frac{\sqrt{\lambda}}{\sigma}\right) \\
&= Q_K\left(\frac{\sqrt{\frac{3}{4} KC}}{\sigma}, \frac{\sqrt{\lambda}}{\sigma}\right), \tag{21}
\end{aligned}$$

where  $Q_K$  is the generalized ( $K$ th-order) Marcum's Q function [18].

## NONCOHERENT CHANNEL COMBINING

In order to avoid wasting signal power during acquisition, the incoming signal can be correlated separately with a local replica of the pilot and the data spreading codes. Noncoherent channel combining is when these correlator outputs are squared and then summed to obtain the decision variable:

$$Z = \sum_{k=1}^K (I_{P,k}^2 + Q_{P,k}^2 + I_{D,k}^2 + Q_{D,k}^2). \quad (22)$$

Similar to the single channel acquisition,  $Z$ , is a chi-square random variable but with  $4K$  degrees of freedom now. When the signal is not present or incorrect delay and Doppler estimates are used,  $Z$  has a central chi-square distribution. When the delay and Doppler estimates are correct,  $Z$  is a non-central chi-square random variable with noncentrality parameter

$$a_{nc}^2 = \frac{3}{4}KC + \frac{1}{4}KC = KC. \quad (23)$$

This leads to the following false alarm and detection probabilities:

$$\begin{aligned} P_{fa}^{nc}(\lambda) &= P(Z > \lambda | H_0) \\ &= \exp\left(\frac{-\lambda}{2\sigma^2}\right) \sum_{k=0}^{2K-1} \frac{1}{k!} \left(\frac{\lambda}{2\sigma^2}\right)^k \end{aligned} \quad (24)$$

and

$$\begin{aligned} P_d^{nc}(\lambda) &= P(Z > \lambda | H_1) = Q_{2K} \left( \frac{a_{nc}}{\sigma}, \frac{\sqrt{\lambda}}{\sigma} \right) \\ &= Q_{2K} \left( \frac{\sqrt{KC}}{\sigma}, \frac{\sqrt{\lambda}}{\sigma} \right). \end{aligned} \quad (25)$$

where  $Q_{2K}$  is the generalized ( $2K$ th-order) Marcum's Q function [18].

Fig. 1 shows the performance of this noncoherent combining detector compared to the single channel and optimal detectors. Semi-coherent integration will attempt to achieve better performance than the noncoherent combining detector to approach that of the optimal detector.

## SEMI-COHERENT INTEGRATION

Semi-coherent integration refers to the noncoherent combination of the 10 ms coherent combinations of the data and pilot components. The pilot and data components can be combined coherently over one spreading code period by using a local composite spreading code

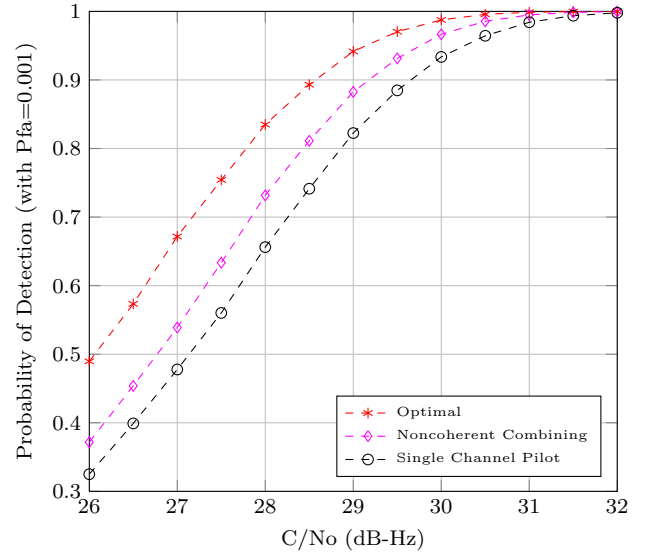


Figure 1: Simulation results that show the detection probability of the Optimal GPS L1C detector, noncoherent combining detector, and single channel pilot detector over two ( $K=2$ ) primary spreading code periods at a fixed false alarm rate of 0.001.

that has the correct relative sign between the data and pilot components:

$$c_P(t)g_P(t) + c_D(t)g_D(t) \quad \text{if } d_P d_D = 1 \quad (26a)$$

or

$$c_P(t)g_P(t) - c_D(t)g_D(t) \quad \text{if } d_P d_D = -1. \quad (26b)$$

Since this relative sign is unknown to the receiver, both these codes are used in coherent channel combining with sign recovery and the correct estimate of the relative sign given by the correlation with the highest power. Subsequent noncoherent combining leads to

$$Z = \sum_{k=1}^K \max \{ |z_k^+|^2, |z_k^-|^2 \}, \quad (27)$$

where

$$z_k^+ = I_{P,k} + jQ_{P,k} + I_{D,k} + jQ_{D,k} \quad (28a)$$

$$z_k^- = I_{P,k} + jQ_{P,k} - I_{D,k} - jQ_{D,k}, \quad (28b)$$

and

$$|z_k^+|^2 = (I_{P,k} + I_{D,k})^2 + (Q_{P,k} + Q_{D,k})^2 \quad (29a)$$

$$|z_k^-|^2 = (I_{P,k} - I_{D,k})^2 + (Q_{P,k} - Q_{D,k})^2. \quad (29b)$$

For the  $K = 1$  case, false alarm and detection probabilities were found in [9] to be:

$$\begin{aligned} P_{fa}^{ch}(\lambda) &= 1 - P(|z^+|^2 < \lambda | H_0) P(|z^-|^2 < \lambda | H_0) \\ &= 1 - \left[ 1 - \exp\left(\frac{-\lambda}{4\sigma^2}\right) \right]^2 \end{aligned} \quad (30)$$



and

$$\begin{aligned}
P_d^{ch}(\lambda) &= 1 - P(|z^+|^2 < \lambda | H_1) P(|z^-|^2 < \lambda | H_1) \\
&= 1 - \left[ 1 - Q_1\left(\frac{\sqrt{(1+\sqrt{3}/2)C}}{\sqrt{2}\sigma}, \frac{\sqrt{\lambda}}{\sqrt{2}\sigma}\right) \right] \\
&\quad \cdot \left[ 1 - Q_1\left(\frac{\sqrt{(1-\sqrt{3}/2)C}}{\sqrt{2}\sigma}, \frac{\sqrt{\lambda}}{\sqrt{2}\sigma}\right) \right]. \quad (31)
\end{aligned}$$

Since the false alarm and detection probabilities easily lead to the cumulative distribution function (CDF), taking the derivative of the CDF gives the probability density function of the decision statistic for  $K = 1$ , under the noise only and signal present cases:

$$f_Z^{K=1}(z; H_0) = \frac{1}{2\sigma^2} \exp\left(\frac{-z}{4\sigma^2}\right) - \frac{1}{2\sigma^2} \exp\left(\frac{-z}{2\sigma^2}\right), \quad (32)$$

$$\begin{aligned}
f_Z^{K=1}(z; H_1) &= \frac{1}{4\sigma^2} \exp\left(\frac{-(1-\sqrt{3}/2)C-z}{4\sigma^2}\right) I_0\left(\frac{\sqrt{(1-\sqrt{3}/2)Cz}}{2\sigma^2}\right) \\
&\quad \cdot \left[ 1 - Q_1\left(\frac{\sqrt{(1+\sqrt{3}/2)C}}{\sqrt{2}\sigma}, \frac{\sqrt{z}}{\sqrt{2}\sigma}\right) \right] \\
&\quad + \frac{1}{4\sigma^2} \exp\left(\frac{-(1+\sqrt{3}/2)C-z}{4\sigma^2}\right) I_0\left(\frac{\sqrt{(1+\sqrt{3}/2)Cz}}{2\sigma^2}\right) \\
&\quad \cdot \left[ 1 - Q_1\left(\frac{\sqrt{(1-\sqrt{3}/2)C}}{\sqrt{2}\sigma}, \frac{\sqrt{z}}{\sqrt{2}\sigma}\right) \right]. \quad (33)
\end{aligned}$$

The characteristic function was found in [10] for the decision variable under  $H_1$  for a slightly less complex probability distribution function due to the equal power split assumption. The characteristic function can then be raised to the power  $K$  to find the characteristic function for the decision statistic for a generic value of  $K$ . In this case, with the unequal power split between the pilot and data components, the probability distribution function contains products of the modified Bessel function and the generalized Marcum's Q function. Numerical techniques be used to find the detection and false alarm probabilities for a given  $K > 1$ .

Fig. 2 shows that this semi-coherent detector does not lead to a detection performance improvement when compared to noncoherent combining. This leads us

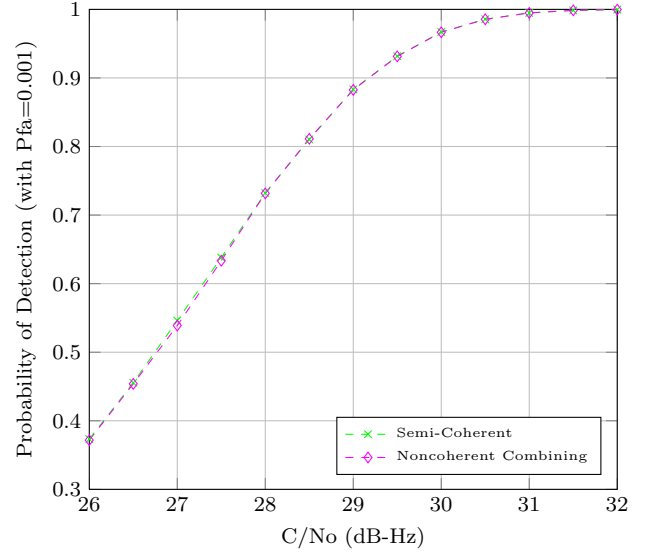


Figure 2: Simulation results that show the detection probability of the semi-coherent and noncoherent combining detectors over two ( $K=2$ ) primary spreading code periods at a fixed false alarm rate of 0.001.

to consider semi-coherent integration in which the unequal power split between the data and pilot components is considered.

### SEMI-COHERENT INTEGRATION WITH UNEQUAL POWER COMPENSATION

The semi-coherent channel combining technique proposed for two component GNSS signals with equal power can be altered to compensate for two-component GNSS signals with unequal power split. The decision variable now incorporates a weighting of each correlator output:

$$Z = \sum_{k=1}^K \max\{|z_k^+|^2, |z_k^-|^2\}, \quad (34)$$

where

$$z_k^+ = \sqrt{\alpha}I_{P,k} + j\sqrt{\alpha}Q_{P,k} + \sqrt{\beta}I_{D,k} + j\sqrt{\beta}Q_{D,k} \quad (35a)$$

$$z_k^- = \sqrt{\alpha}I_{P,k} + j\sqrt{\alpha}Q_{P,k} - \sqrt{\beta}I_{D,k} - j\sqrt{\beta}Q_{D,k}, \quad (35b)$$

and

$$|z_k^+|^2 = \left(\sqrt{\alpha}I_{P,k} + \sqrt{\beta}I_{D,k}\right)^2 + \left(\sqrt{\alpha}Q_{P,k} + \sqrt{\beta}Q_{D,k}\right)^2 \quad (36a)$$

$$|z_k^-|^2 = \left(\sqrt{\alpha}I_{P,k} - \sqrt{\beta}I_{D,k}\right)^2 + \left(\sqrt{\alpha}Q_{P,k} - \sqrt{\beta}Q_{D,k}\right)^2, \quad (36b)$$

with

$$\alpha = \frac{3}{4} \quad \text{and} \quad \beta = \frac{1}{4}.$$

For the  $K = 1$  case, false alarm and detection probabilities were found in [9] to be:

$$\begin{aligned} P_{f_a}^{chw}(\lambda) &= 1 - P(|z^+|^2 < \lambda | H_0) P(|z^-|^2 < \lambda | H_0) \\ &= 1 - \left[ 1 - \exp\left(\frac{-\lambda}{2\sigma^2}\right) \right]^2 \end{aligned} \quad (37)$$

and

$$\begin{aligned} P_d^{chw}(\lambda) &= 1 - P(|z^+|^2 < \lambda | H_1) P(|z^-|^2 < \lambda | H_1) \\ &= 1 - \left[ 1 - Q_1\left(\frac{\sqrt{C}}{\sigma}, \frac{\sqrt{\lambda}}{\sigma}\right) \right] \\ &\quad \cdot \left[ 1 - Q_1\left(\frac{\sqrt{\frac{1}{4}C}}{\sigma}, \frac{\sqrt{\lambda}}{\sigma}\right) \right]. \end{aligned} \quad (38)$$

The probability density functions of the decision statistic for  $K = 1$  under both the noise only and signal present cases are

$$f_Z^{K=1}(z; H_0) = \frac{1}{\sigma^2} \exp\left(\frac{-z}{\sigma^2}\right) - \frac{1}{\sigma^2} \exp\left(\frac{-z}{\sigma^2}\right), \quad (39)$$

$$\begin{aligned} f_Z^{K=1}(z; H_1) &= \frac{1}{4\sigma^2} \exp\left(\frac{-(1-\sqrt{3}/2)C-z}{4\sigma^2}\right) I_0\left(\frac{\sqrt{(1-\sqrt{3}/2)Cz}}{2\sigma^2}\right) \\ &\quad \cdot \left[ 1 - Q_1\left(\frac{\sqrt{(1+\sqrt{3}/2)C}}{\sqrt{2}\sigma}, \frac{\sqrt{z}}{\sqrt{2}\sigma}\right) \right] \\ &\quad + \frac{1}{4\sigma^2} \exp\left(\frac{-(1+\sqrt{3}/2)C-z}{4\sigma^2}\right) I_0\left(\frac{\sqrt{(1+\sqrt{3}/2)Cz}}{2\sigma^2}\right) \\ &\quad \cdot \left[ 1 - Q_1\left(\frac{\sqrt{(1-\sqrt{3}/2)C}}{\sqrt{2}\sigma}, \frac{\sqrt{z}}{\sqrt{2}\sigma}\right) \right]. \end{aligned} \quad (40)$$

Numerical techniques can be used to find the detection and false alarm probabilities for a particular  $K > 1$  from (39) and (40).

The improvement in detection performance of semi-coherent integration when compensated for the unequal power split between the data and pilot components is shown in Fig. 3.

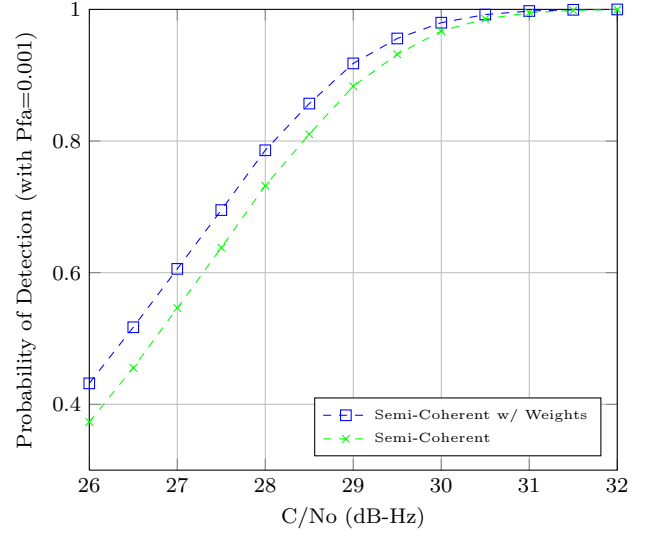


Figure 3: Simulation results that show the detection probability of semi-coherent integration with and without compensating for the data/pilot power split over two ( $K=2$ ) primary spreading code periods.

## PERFORMANCE AND COMPARISON

In this section, results from various simulations are presented. Specifically, we focus on the detection probabilities of the various acquisition schemes discussed at a fixed false alarm rate of 0.001. As shown in Fig. 4 and also discussed in [9], performance of semi-coherent integration with unequal power compensation approaches that of the optimal detector over one spreading code period,  $K = 1$  (no noncoherent combinations are used).

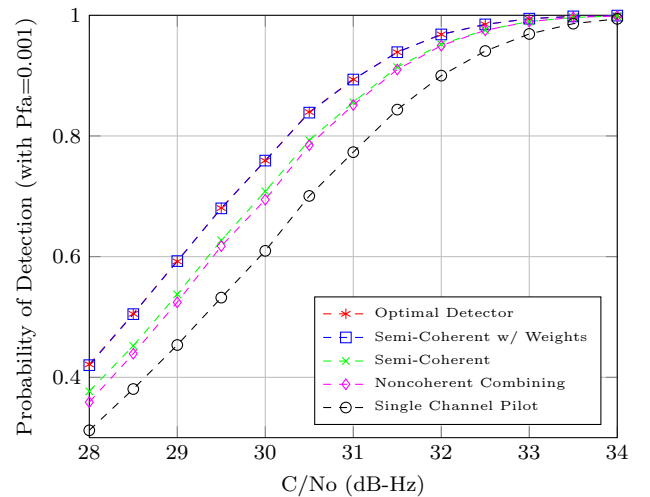


Figure 4: Simulation results that show the detection probability of various GPS L1C acquisition schemes over one ( $K=1$ ) primary spreading code period.

Once multiple spreading code periods are used ( $K > 1$ ), the performance of semi-coherent integration with unequal power compensation no longer achieves the optimal detector's performance but its still greater than that of the noncoherent combining detector as shown in Fig. 5 and Fig. 6.

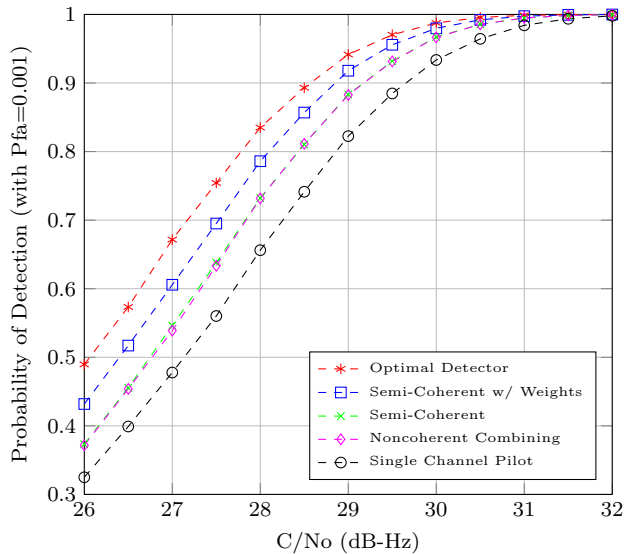


Figure 5: Simulation results that show the detection probability of various GPS L1C acquisition schemes over two ( $K=2$ ) primary spreading code periods.

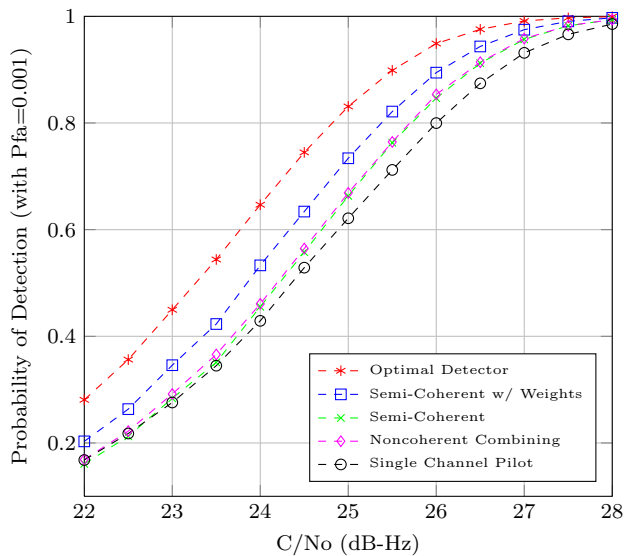


Figure 6: Simulation results that show the detection probability of various GPS L1C acquisition schemes over five ( $K=5$ ) primary spreading code periods.

To determine if semi-coherent integration with unequal power compensation would still provide the slight per-

formance improvement over noncoherent combining with extended total integration times, Figs. 7 and 8 show the detection probabilities for  $K=10$  and  $K=20$  respectively.

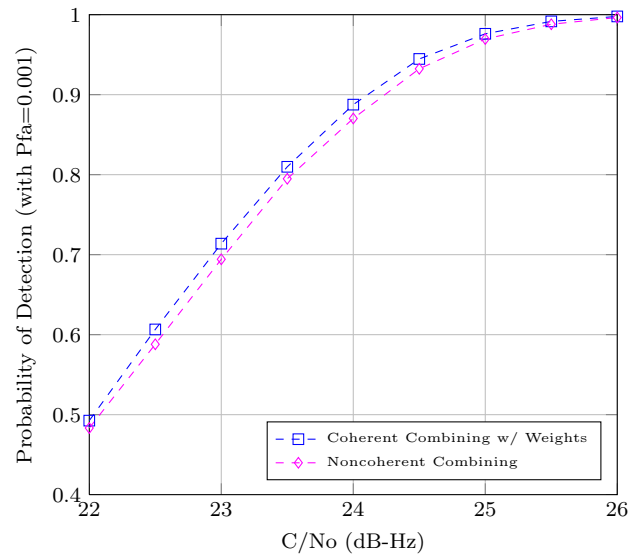


Figure 7: Simulation results that show the detection probability of semi-coherent integration with unequal power compensation and noncoherent combining over 10 primary spreading code periods ( $K=10$ ).

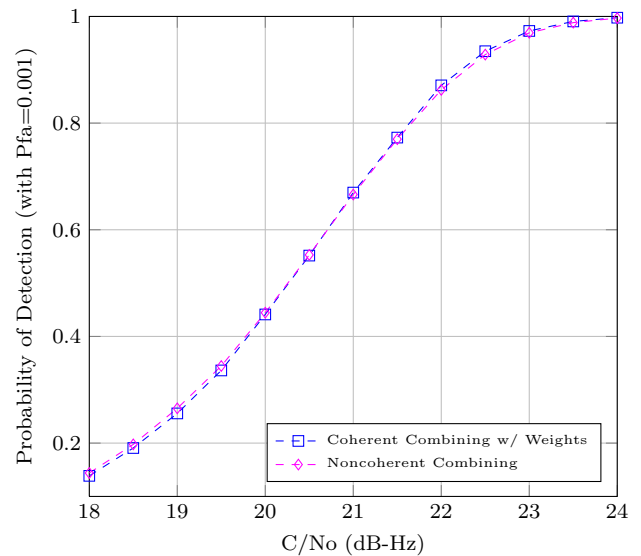


Figure 8: Simulation results that show the detection probability of semi-coherent integration with unequal power compensation and noncoherent combining over 20 primary spreading code periods ( $K=20$ ).

Semi-coherent integration with unequal power compensation retains its performance advantage over non-

coherent combining until using twenty spreading code periods or a Carrier-to-Noise ratio of 23 dB-Hz.

## CONCLUSIONS

The GPS L1C signal like most modern GNSS signals has both a pilot and data component but with the unique aspect of an unequal power split between the two components. The optimal detector for GPS L1C acquisition over multiple spreading code periods without knowledge of the navigation data and overlay code phase was derived. In addition, noncoherently adding the coherent combinations of the pilot and data components, or semi-coherent integration, was investigated. Semi-coherent integration was shown to provide a detection performance improvement (about 0.4 dB) over noncoherent combining when compensated for the unequal power split between the data and pilot components. Simulations show the performance of semi-coherent integration compared to the optimal detector, noncoherent combining, and pilot channel only acquisition.

## REFERENCES

- [1] F. Bastide, O. Julien, C. Macabiau, and B. Roturier, "Analysis of L5/E5 acquisition, tracking and data demodulation thresholds," *ION GPS 2002*, September 2002.
- [2] C. Hegarty, M. Tran, and A. J. V. Dierendonck, "Acquisition algorithms for the GPS L5 signal," *ION GPS/GNSS 2003*, September 2003.
- [3] D. Borio, C. O'Driscoll, and G. Lachapelle, "Coherent, noncoherent, and differentially coherent combining techniques for acquisition of new composite GNSS signals," *Aerospace and Electronic Systems, IEEE Transactions on*, vol. 45, no. 3, pp. 1227–1240, July 2009.
- [4] A. J. V. Dierendonck and J. J. J. Spilker, "Proposed civil GPS signal at 1176.45 MHz: In-phase/quadrature codes at 10.23 MHz chip rate," *ION 55th Annual Meeting*, June 1999.
- [5] C. J. Hegarty, "Optimal and near-optimal detectors for acquisition of the GPS L5 signal," *ION National Technical Meeting 2006*, January 2006.
- [6] C. Yang, C. Hegarty, and M. Tran, "Acquisition of the GPS L5 signal using coherent combining of I5 and Q5," *ION GNSS 17th International Technical Meeting of the Satellite Division*, September 2004.
- [7] P. G. Mattos, "Acquisition of the Galileo OAS L1B/C signal for the mass-market receiver," *ION GNSS 18th International Technical Meeting of the Satellite Division*, 2005.
- [8] —, "Galileo L1C - acquisition complexity: Cross correlation benefits, sensitivity discussions on the choice of pure pilot, secondary code, or something different," *IEEE*, 2006.
- [9] K. C. Seals, W. R. Michalson, P. F. Swaszek, and R. J. Hartnett, "Analysis of coherent combining for GPS L1C acquisition," *ION GNSS 2012*, September 2012.
- [10] D. Borio, C. O'Driscoll, and G. Lachapelle, "Composite GNSS signal acquisition over multiple code periods," *Aerospace and Electronic Systems, IEEE Transactions on*, vol. 46, no. 1, pp. 193–206, Jan. 2010.
- [11] J. Betz, M. Blanco, C. Cahn, P. Dafesh, C. Hegarty, K. Hudnut, V. Kasemsri, R. Keegan, K. Kovach, L. Lenahan, H. Ma, J. Rushanan, J. Rushanan, D. Sklar, T. Stansell, C. Wang, and S. Yi, "Description of the L1C signal," *Proceedings of the 19th International Technical Meeting of the Satellite Division of The Institute of Navigation (ION GNSS 2006)*, pp. 2080–2091, September 2006.
- [12] T. Stansell, K. Hudnut, and R. Keegan, "GPS L1C: Enhanced performance, receiver design suggestions, and key contributions," *23rd International Technical Meeting of the Satellite Division of The Institute of Navigation*, 2010.
- [13] SAIC, "Navstar GPS space segment / user segment L1C interface, IS-GPS-800a," Science Applications International Corporation, Tech. Rep., June 8, 2010.
- [14] J. J. Rushanan, "The spreading and overlay codes for the L1C signal," *NAVIGATION: Journal of The Institute of Navigation*, vol. 54, no. 1, pp. 43–51, 2007.
- [15] J. W. Betz, "Binary offset carrier modulations for radionavigation," *Navigation: Journal of the Institute of Navigation*, vol. 48, no. 4, pp. 227–246, March 2002.
- [16] P. Misra and P. Enge, *Global Positioning System: Signals, Measurements and Performance*, revised second edition ed. Lincoln, MA: Ganga-Jamuna Press, 2011.
- [17] H. L. V. Trees, *Detection, Estimation, and Modulation Theory Part I*. Wiley, 1968.
- [18] J. G. Proakis, *Digital Communications*. McGraw Hill, 2001.